PROCEEDINGS OF SCIENCE

https://pos.sissa.it/

PoS(ICRC2023)034

Rapporteur Talk: Solar and Heliospheric

Agnieszka Gil *a,b* *

a Siedlce University,
Konarskiego 2, Siedlce, Poland

b Space Research Centre, Polish Academy of Sciences,
Bartycka 18A, Warsaw, Poland

E-mail: gila@uph.edu.pl

This rapporteur paper summarizes the 127 contributions on solar and heliospheric physics (i.e. the SH sessions) presented during the 38th International Cosmic Ray Conference in Nagoya. Presented works covered a range of topics concerning updates on methods and instruments allowing cosmic rays measurements. Progress done in the modeling of modulation, acceleration and propagation of cosmic rays within the heliosphere was discussed. During the oral presentations and posters variety of topics were discussed. Among them there were deliberated such topics as changeability observed in the galactic cosmic rays (GCR) flux on the ground, i.e. GCR diurnal anisotropy, Forbush decreases, mid-and long-term GCR periodicities. Solar energetic particles (SEP) and ground level enhancements (GLEs) observational and modeling results were presented. Calculation of radiation dose for airplane passengers and crew, as well as astronaut, were reported. Moreover, historical reconstructions were discussed.

38th International Cosmic Ray Conference (ICRC2023)
26 July - 3 August, 2023
Nagoya, Japan

ICRC2023
38th International Cosmic Ray Conference
The Astroparticle Physics Conference

*Speaker

1. Introduction

It was a great honor to be invited to summarize solar-heliospheric (SH) sessions of the 38th International Cosmic Ray Conference. I would like to express my great gratitude to all the Authors of the presentations, who reported their results in an extremely interesting and comprehensive manner. Discussions were fascinating and in-depth. Moreover, the need of a personal meeting after the pandemic break was very clearly visible, especially bearing in mind, that we participated in the previous ICRC remotely.

The leading topic of all presented talks and posters were, of course, changes occurring in the behavior of the cosmic ray flux under the influence of solar activity. Phenomena originating on the Sun such as solar wind, heliospheric magnetic field, coronal mass ejections, solar energetic particles, coronal holes, etc. are reflected in the level and behavior of the observed cosmic rays. Particles which are propagating and accelerated in the heliosphere, especially solar energetic particles and their space weather impacts on Earth were a subject of many presentations. Nowadays we have an extraordinary opportunity thanks to Parker Solar Probe and Solar Orbiter learning about the Sun and heliosphere. Acceleration and propagation processes can be studied in such close proximity to Sun as never before. What is particularly noteworthy is that the news regarding the latest observations have not only come from instruments on various space missions, but also a lot is happening in the field of ground-based observations. Progress made in modeling solar energetic particles acceleration, heliospheric transport of cosmic rays, and galactic cosmic rays variability mathematical modeling were delivered.

This article is organized in the following way: the Second Section describes Instrumentation, new one and upgrades; the Third Section is devoted to the subject of radiation environment at Earth and the Fourth one to the historical reconstructions and observations. The Fifth Section concentrates on the topic of Solar Energetic Particles events. The Sixth and Seventh Sections deliver our updates on Solar Modulation of Galactic Cosmic Rays, observational and modeling, respectively. In the next Section the short Summary is given. Although, it has to be underlined, that the topics of these sections interpenetrate each other, making it inevitable to return to some issues throughout the review.

2. Instrumentation

2.1 In space observations

Learning about the Sun and heliosphere is nowadays supported by many assets. Acceleration and transport processes are intertwined in distant observations [1]. Currently we have information about the state of space in such distant places, outside the heliosphere, as the Voyager probes locations: ~164 AU Voyager 1 and ~134 AU Voyager 2, up to as close to the Sun as Solar Orbiter: ~0.31 AU, and Parker Solar Probe: ~0.02 AU (Figure 1).

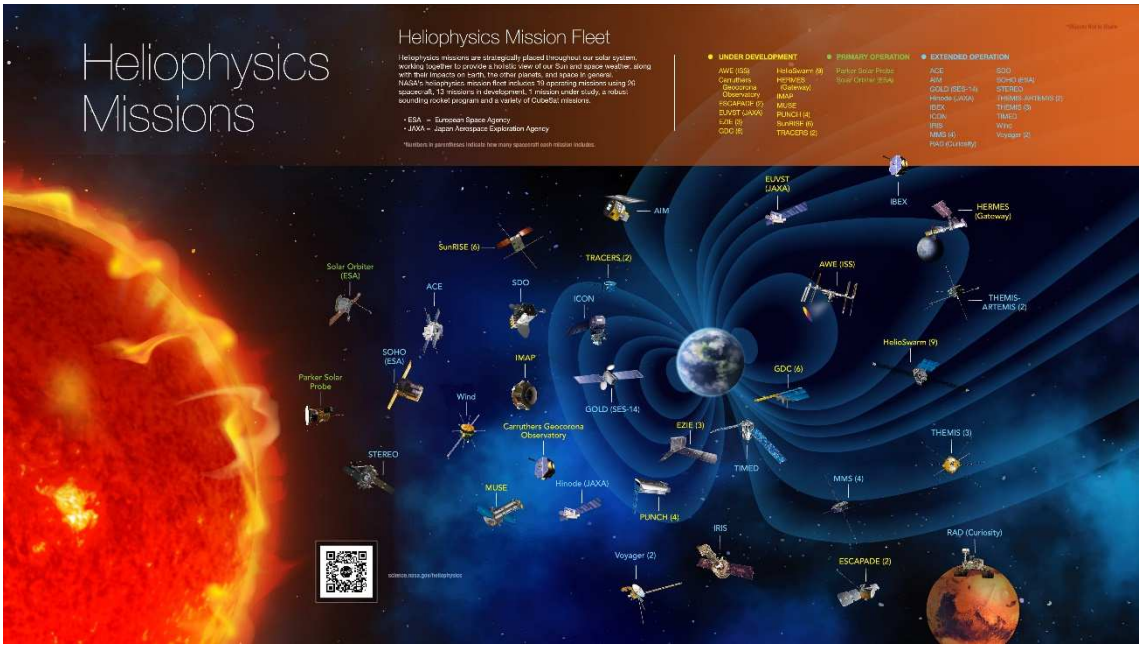

Figure 1. Heliophysics spacecraft in orbit. State for 14.03.2023 (https://science.nasa.gov/)

Solar Orbiter (SolO) was launched on 10.02.2020. It will achieve perihelion of 0.3 AU and 24° latitude [2]. Parker Solar Probe (PSP) was launched on 12.08.2018 and it will achieve perihelion at distance less than 10 solar radii (R_S) [3]. As a future perspective: SolO will go out of ecliptic plane and PSP is getting closer to the Sun, all this while the solar activity increases.

One of the important subject of the SH sessions were unique observations made by those two state-of-the-art missions. Acceleration and transport highlights were given, among them evolution of turbulence from 0.1 to 1 AU, with radial alignment of Parker Solar Probe and Solar Orbiter shown. Solar energetic particles (SEPs) onset, anisotropy and shock connection analysis were presented. During these five years from launch the Integrated Science Investigation of the Sun (IS⊙IS) instrument has made numerous SEP events observations. One of them, highly anisotropic, happened on 05.09.2022 observed from the distance smaller than 17 R_S. This SEP event was associated with a fast CME and a soft strong X-ray flare [4]. It was reported as the one with exceptionally low Fe/O ratios, with heavy ions reaching the maximum intensities about 5 orders of magnitude larger than GCRs at energy 10 MeV/n and with much harder spectra.

There were also observed many 3He-rich SEP events. Properties of two of them, on 21.01.2021 and 30.05.2022, such as, much softer spectrum for 3He than for 4He for energies being above 1 MeV/nuc, were discussed [5]. Moreover, the response matrix approach of electron spectra estimation was presented for the 05.09.2022 event observed by EPI-Hi HET instrument on board of the Parker Solar Probe [6].

The Alpha Magnetic Spectrometer (AMS-2) since 19.05.2011 has collected two helium SEP events (one of them on 11.09.2017) and 28 proton SEP events. These events were connected with M- and X-class solar flares, and fast CMEs. It was reported that the most energetic events in the AMS-2 SEP list are these helium events [7].

Strong G3 geomagnetic Storms were observed by the High-Energy Particle Detector, HEPD-01, on 26.08.2018 and 12.05.2021. There were reported spectra of the re-entrant leptons

(20-100 MeV), and also proton fluxes (40-250 MeV) inside the South Atlantic Anomaly [8]. In total 9 SEP events were detected by HEPD-01, among them the one on 28.10.2021. It was a source of the first Ground Level Enhancement (GLE) of Solar Cycle (SC) 25, namely GLE 73 (Figure 2).

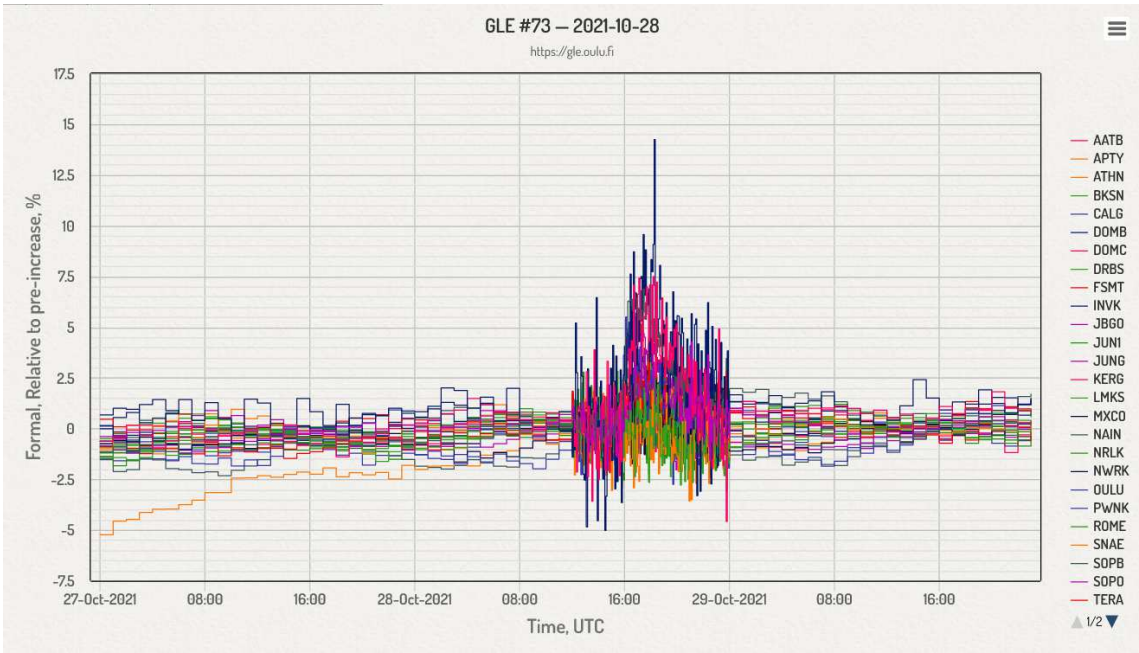

Figure 2. GLE 73 on 28.10.2021 as observed on the ground by the neutron monitors (https://gle.oulu.fi)

It was reported that based on the HEPD-01 data combined with the Electron Proton and Alpha Monitor (EPAM, onboard on the Advanced Composition Explorer (ACE), the Electron Proton and Helium Instrument (EPHIN) and the Energetic and Relativistic Nuclei and Electron (ERNE) (both onboard of the Solar and Heliospheric Observatory, SOHO) experiments measurements time-integrated proton spectrum for this event was estimated [9]. A new design for Tracker Data AcQuisition (TDAQ) system of the HEPD-02, a particle spectrometer, on a board of the China Seismo-Electromagnetic Satellite has been presented [10-11].

Since solar neutrons are important observation probes to understand solar ion acceleration mechanisms, there was presented a new instrument for microsatelites, SOlar Neutron and Gamma-ray Spectrometer. It is planned to be sensitive to both fast neutrons and soft gamma-rays. Its launch is aimed around 2025 as one of the payloads on board the 5th JAXA satellite [12].

The possibilities to observe behaviour of various species of particles, among them: electrons-within radiation belt, and outside-mostly primary protons in a Sun-synchronous orbit by the ASO-S, operating at 720 km altitude were described [13-14].

2.2 Suborbital observations

The balloon-borne spectrometer AESOP-Lite (Anti-Electron Sub-Orbital Payload Low Energy) observed a time difference in the diurnal geomagnetic cutoff transitions between

electrons and positrons, at energies between 20 MeV and 300 MeV during its 05.2018 flight from Kiruna in Sweden to Ellesmere Island in Canada [15].

2.3 On the ground measurements

Numerous reports have addressed the updates and observations made by neutron monitors (NMs), which are instruments situated on the ground designed to detect secondary particles. The secondary GCRs are generated in the atmosphere due to the interactions with its molecules. NMs are particularly sensitive to secondary neutrons, originating from primary cosmic rays within the GeV energy spectrum [16]. The response of these detectors to primary cosmic rays is significantly influenced by Earth's magnetic field, which effectively acts as a spectrometer. Specific geographical locations across the globe are characterized by a geomagnetic cutoff, measured in GV. This threshold determines the ability of ground-based detectors to register cosmic rays. Its value varies from less than 1 GV in the polar regions up to 17 GV in Thailand. To enable the detection of atmospheric secondary particles at ground level, the particle's rigidity must also surpass a separate atmospheric cutoff of 1 GV. Given the location-dependent nature of the above described cutoff values, neutron monitors have been deployed in numerous locations worldwide (Figure 3), also at various altitudes, up to high mountains. In this contexts, works performed on the redeploying the Haleakala NM, on the Maui island, which were reported are important for filling a gap in the global NM network, at the Pacific Ocean region [17].

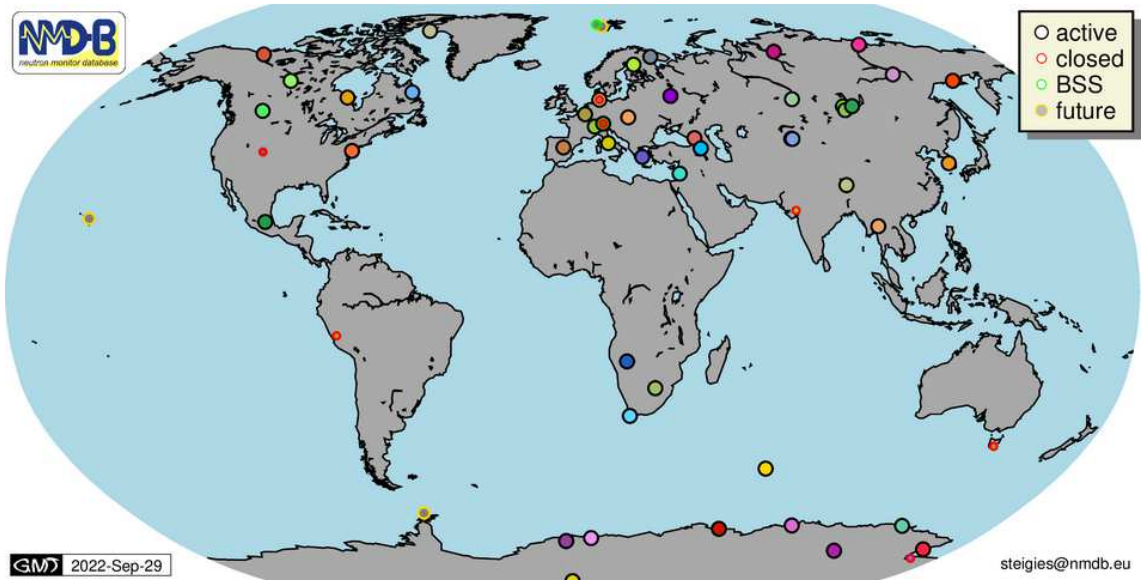

Figure 3. Neutron Monitor stations at Neutron Monitor DataBase (www.nmdb.eu)

Several reports were devoted to the so called 'leader fraction' measurements. It is neutron counts fraction that didn't track another linked (in time) neutron count originating from the same primary CR. It was discussed that the leader fraction can be used as an indicator of the GCR spectral index variations, based on the calibration from the South Pole NM, with a daily spectral index originating from AMS-02 GCR proton fluxes, for the period of 2015-2019 [18]. That

allowed to conclude that NM network is capable to conduct accurate and uninterrupted monitoring of GCR spectral variability. The rigidity spectrum exponent gamma of GCR intensity variation computed for the period of 2009–2019 exhibited the soft rigidity spectrum around near solar activity (SA) maximum, while near the SA minimum it was hard [19]. Authors propose that spectral index gamma can be considered as a natural proxy of the long-term GCR variations. Other report was concerned on the usage of NMs as a calorimeter to measure particle spectra [20]. These results were compared with the leader fraction, as a GCR spectral index proxy.

Utilization of bare neutron counters, which operate without the lead producer and polyethylene reflector at Mawson NM, was presented in the context of a better comprehension of the yield functions and spectral index determination [21]. Mawson NM was also used for comparison with latitudinal surveys in the studies of the polarity effect visible in the NMs measurements [22]. The simulated differential response function was compared with measurements performed during the latitudinal survey in 2019 (Figure 4) [23]. It allowed to investigate differences in the response function between the two leaded edge tubes and the unleaded middle tube (where all three counters were inside the same reflector). This report once again emphasized the importance of the latitudinal surveys.

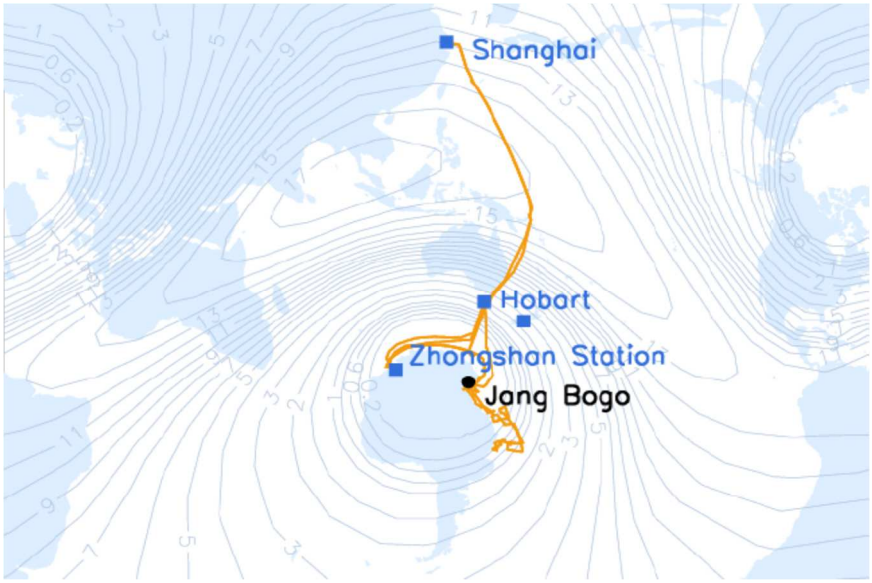

Figure 4. Path of Changvan in the 2019 latitudinal survey year is marked by the orange line. The contour lines with accompaning numerical values mean the vertical cutoff rigidity, in GV, calculated for 11.02.2019, at 12:00 UT [23].

The high cut off rigidity Princess Sirindhorn Neutron Monitor cross-counter leader fraction allowed to analyze a dependence on NM tubes separation and differences between end and middle counters [24]. Based on the same NM properties, such as nuances originating from various counter efficiencies, the possibility of the extent and features of air showers studies was reported [25]. Simulation of neutron bursts originating from air shower cores interacting in ice results were reported [26]. In this context also fluences analysis performed based on the South Pole NM observations were discussed.

Issue of the declining trend in the South Pole NM data were discussed based on the Monte Carlo simulation results [27]. It was summarized that to resolve this require continuous measurements for at least one more SC.

Due to the full transfer of McMurdo NM to Jang Bogo completed in 2017 the cross-correlation between these two NMs was studied [28]. The time lags for these two NMs data-sets were estimated and given in the interval: −172800 to +172800 seconds.

There was a report about new Boron Trifluoride proportional tube for the NM64 Neutron Monitor, being suitable for a replacement of the original BP28 (Figure 5), which are no longer produced [29]. The satisfying efficiency assessments were presented for tubes with higher cathode thickness, with the same or lower anode wire diameter, as well as for lower operating voltage.

Figure 5. Photos of the LND-BP28 from Sharp Laboratory at the University of Delaware. On the right photo are shown the locations of the measurements alongside with an original BP28 [29]

The first results from the Izaña Cosmic Ray Observatory (ICaRO), based on the ORCA design, i.e. with complimentary neutron monitor and muon telescope, were reported [30]. This observatory is located at high altitude, 2373 m, with vertical cut-off rigidity being equal 11.5 GV.

There was also discussed the detection efficiency and energy deposition for a new detector of the Sierra Negra Cosmic Rays Observatory, at 4580 m altitude: the Scibar Cosmic-Ray Telescope (SciCRT). Its design supports to observe solar neutrons and the muon background produced by GCRs [31]. Measurements performed during intense and moderate geomagnetic storms in the period of 12.2015-12.2022 allowed to report that noticeable decreases in the counting rate of at least one Solar Neutron Telescope channel were visible [32]. Moreover, properties of solar neutron decay protons, being infrequent events, were discussed [33]

Since the end of 2022 in the Cosmic ray Laboratory at Chacaltaya in Bolivia, at altitude of 5240 m, a bonner sphere neutron spectrometer and dosimetric instruments operate in the frame of South Atlantic Magnetic Anomaly Dosimetry at High Altitude (SAMADHA) project. In the South Atlantic Anomaly region the secondary cosmic ray neutrons spectrum as well as an environmental dose owing to GCRs at very high elevation are monitored [34].

The role of the GRAPES-3 experiment in contributing to the space weather studies of the transit of geomagnetic storm from lagrangian point L1 to Earth's surface was discussed [35]. Presented results were based on the analysis of the severe, G4 geomagnetic storm on 22.06.2015,

which was triggered by the massive CME. It was also introduced that join observations of GRAPES-3 and Akeno muon telescopes may bring a more comprehensive insight into the 3-D configuration of solar wind and its impacts in the heliosphere [36].

The Large High Altitude Air Shower Observatory (LHAASO), at the altitude of 4 410 m, can detect air showers originating from cosmic rays with GeV to PeV energies. Based on the sky-maps relative to LHAASO zenith, a method of studies of GCR transient effects was shown [37]. As an example, using the CME passage on 4-5.11.2021, an enhanced anisotropy was reported.

Muon tomography technique, using a directional flux of GCR muons as a source to scan the density variation of objects was presented [38].

2.3.1 Terrestial Gamma Rays

An intense downward terrestrial gamma-ray flash (TGF) was registered on 24.11.2017, at the Kashiwazaki-Kariwa nuclear power plant, during a lightning discharge. As it was reported, TGF triggered atmospheric photonuclear reactions, resulting in the neutrons production. There were also noticed radiation dose enhancements due to this TGF [39].

2.3.2 Sun Shadow Cosmic Rays

Cosmic rays striking the Sun are the subject of absorption leading to the creation of a cosmic ray shadow that has been detected and studied in the air-shower observations. The high energy protons (TeV range) are unmodulated at Earth's orbit but can be considerably deflected by the strong magnetic fields close to the Sun. Moreover, cosmic rays can also interact with matter near the solar surface creating gamma ray. These two aspects were reported with a simple model of the Sun including regions of closed and open magnetic fluxes [40].

Predictions of the heliospheric magnetic field By component changes up to three days using the cosmic ray (at the energy range around 40 TeV) Sun shadow as observed by the LHAASO-KM2A were deliberated [41].

2.3.3 Synchrotron Radiation

Based on the precise GCR electron measurements with up to date solar and heliospheric magnetic field observations estimates of the synchrotron emission from gamma rays to radio in the direction of the Sun and in the heliosphere produced by GCR electrons in the solar magnetic field have been reported [42]. Modeled synchrotron profile displayed that it practically doesn't change within the solar disk, it reach the highest level in the Sun's proximity, where the magnetic field is maximal, and next quickly falls away from the solar surface.

2.3.4 Solar-Flare Neutrino

There was presented a method of usage of a Cherenkov neutrino telescope KM3NeT for solar-flare neutrino explorations in the MeV-GeV energy range [43].

2.3.5 Some Aspects of Space Weather

Various practical aspects of space weather were discussed based on data from ground-based equipment: a global network of the ground-based multidirectional muon detectors (the Global Muon Detector Network, GMDN) and neutron monitors data, such as situation when 38 of the 49 Starlink satellites launched on 03.02.2022 re-entered the atmosphere [44] or electrical grid failures [45]. There were also presented studies of the CMEs-driven GCR variation having no direct effect on Earth [46]. The magnetic cloud orientation was discussed in the case of the CME on 3.10.2012 [47].

3. Radiation Environment at Earth and near Earth

Several reports have discussed the findings in the field of the radiation environment and its impacts.

Taking into account that aircraft passengers and crew experience increased radiation exposure compared to the sea level, reliable and precise models are needed. Application COde for the Radiation Dose Estimation, ACORDE, tool was discussed, based on computations made for over 300 flights. These also included flights falling during the period of GLE 73 [48]. Estimations of the effective dose at flight heights during fifteen GLEs, among them the two strongest ones: GLEs 5 and 69 were presented. A new radiation model, utilizing time-dependent SEP spectra, was their basis [49]. It was reported that a potential proxy of a dose could be determined based on the NMs data, helping in now-casting, and mitigation of the potential GLE hazards. It was shown that the impact of GLE 73 was rather slight with a maximal relative rise in a dose above the GCR background of ≈30% noticed in the polar regions, thus this event would be responsible for only a minor amount of the average passengers and crew annual exposure. The effect of GLE 73 in equatorial regions was discussed as insignificant [50]. Computations of the spectra and angular distribution of GLE 60 were presented in the context of their importance for the aviation dosimetry [51]. A comparison of the modeling results and measurements were presented. These calculations were based on the newly developed open-source tool for computing cosmic ray trajectories in the Earth's magnetosphere [52]. There was also reported a new model serving for calculation of astronaut radiation dose [53].

The primary spectrum of GLE 71 obtained based on the NMBANGLE PPOLA model was reported [54], being in an agreement with Payload for Antimatter Matter Exploration and Light-nuclei Astrophysics (PAMELA) data. It was suggested that particles being the source of this GLE were injected at the footpoints of the propagating magnetic cloud.

4. Historical observations

The cosmogenic isotopes, allows for quantitative analysis of solar and cosmic-ray changeability over long-timescales (e.g. [55]).

A systematic reconstruction of integral fluences for four historical extreme solar particle events on 994 CE, 775 CE, 660 BCE, and 7176 BCE was presented [56]. Authors reported that fluences are an order of magnitude higher for energies lower than 100 MeV in comparison to previously estimated.

Global map of the integrated ambient dose at altitude 40 kft for the strongest ever observed event (based on cosmogenic radionuclides records) in 774 AD was presented for the two differing scenarios: a conservative with hard spectra scaled from GLE 5, and a realistic with softer spectra from GLE 45 were reported (Figure 6) [57].

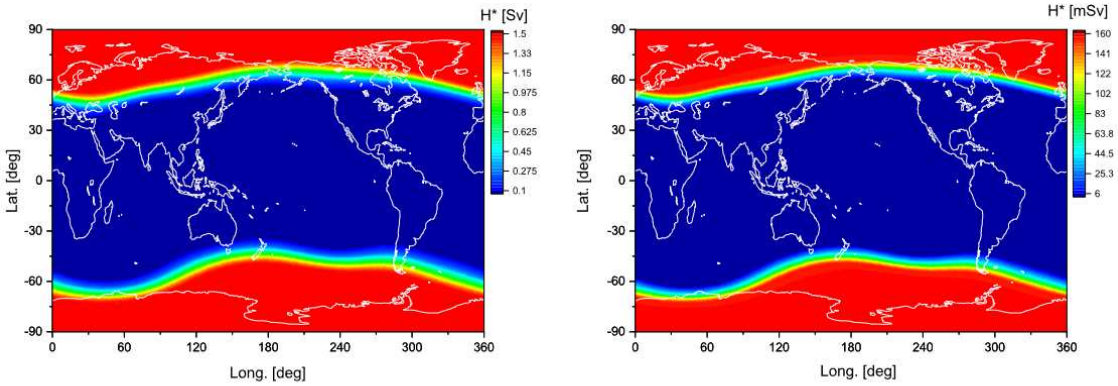

(a) Worst case scenario **(b)** Realistic scenario

Figure 6. Global map of the integrated ambient dose at altitude 40 kft over the first 6h starting from the event onset during 774 AD event [57].

Based on the cosmogenic isotope 14C concentrations in tree rings in the 19th century it was discussed that any substantial concentration growth related to the extreme geomagnetic storms wasn't confirmed. It suggests that no measureable SEP events appeared during the measurement time interval [58].

Historical observations of the first four GLEs were reported [59]. The significant improvement of the temporal resolution and geographical coverage was shown, allowing for the studies of spectral and angular events characteristics. One of the features revealed in this study was that GLE 2 and 4 might have a similar spectra.

Ion chambers (ICs) historical records where used in order to assess the SEP spectra during the GLE 4, the strongest event recorded during the pre-NM era [60]. Moreover, modulation parameters of GCR transport in the heliosphere based on the GCR anisotropy were estimated based on the ICs data [61]

A careful examination of the NMs data from the period 03.1964-12.1969 allowed to find two sub-GLE events: on 09.06.1968 and on 27.02.1969 with the enhanced count rate of South Pole and Vostok NMs [62].

5. Solar energetic particles events analysis

5.1 SEP observational results

It was reported that the direct data from the space era do not accurately depict the long-term average of solar energetic particle flux. This is because they account for only 20-55% of the total, with the majority being attributed to rare, extremely intense SEP events from the past [63]. Taking into account both, direct (from GOES) and proxy data (from cosmogenic isotopes 14C, 10Be and 36Cl), harmonious correspondence with the mega-year averaged one, was shown. This alignment

demonstrated that comprehension of the complete range of SEP flux, encompassing common events to sporadic extreme occurrences, is fully consistent.

Annual SEP fluences during 1984–2019 demonstrating variations over the SC, were shown, with SC 24 exhibiting considerably smaller fluences in comparison to SCs 22 and 23 [64]. These results were based on the revised calibration of GOES data.

Investigations of the sub-populations within the Fermi-LAT catalogue of gamma-ray solar flares, based on measurements of the X-ray and γ-ray fluxes, as well as CMEs and SEPs, were reported [65].

The key role of the perpendicular diffusion effects was suggested, rather than interplanetary shocks, in the longitudinal distribution of most gradual SEP [66].

5.2 SEP modeling

It was discussed that SEP prediction models have several requirements as: magnetic field realistic model and structure of the plasma, shape, size and propagation of CME shock, as well as injection of accelerated SEP particles. Reported results showed that the absolute SEP flux level, time profiles, and anisotropy can be satisfactorily predicted [67].

New developments and future plans in the SEPCaster simulations of the transport and acceleration in gradual SEP events were presented [68]. Particle acceleration described in 1-D modeling showed the flattening of the spectra from escape at higher energies and the trapping at low energies [69]. There was proposed a model of SEP origination from the solar loop termination shock [70].

Monte Carlo approach for studies of the energy spectrum in the case of the twin flare event was presented, when quasi-parallel shocks related with a large SEP event appeared [71].

Spatial variation of the magnetic field path lengths impact on SEP transport based on the Monte Carlo simulations with 2D magnetic field with slab fluctuation was reported [72]. Differences for impulsive solar flares, with narrow solar injections and gradual SEP events, with wide injections, were shown.

1D particle-in-cell simulations of quasi-perpendicular shocks were discussed in the context of the electron acceleration efficiency in the relation to the whistler critical Mach number [73].

5.3 SEE observational results

Possible evolutions of solar energetic electron (SEE) events spectrum, based on the analysis of measurements from WIND at 1AU, during the period 12.1994-12.2019, were reported [74].

The release times and their energy dependences of near-relativistic electrons in the case of impulsive SEE events, that have been subjected to statistical study, have been presented [75].

6. GCR solar modulation in various time-scales

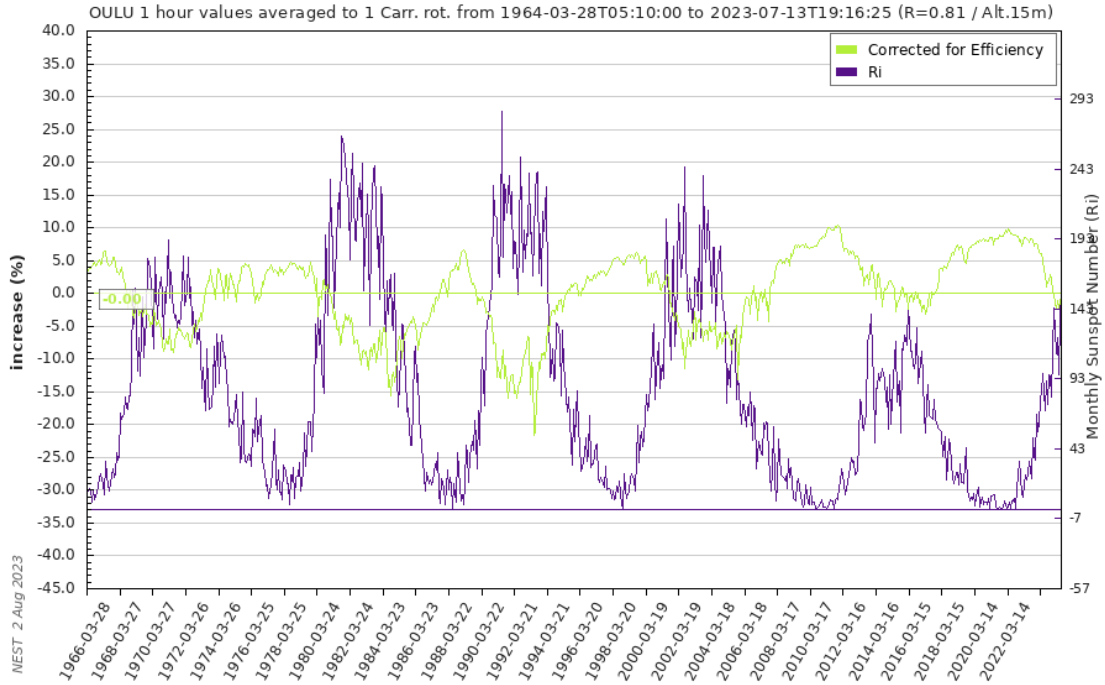

Figure 7. Solar modulation of GCR with clear 11-year variation in GCR count rates (https://www.nmdb.eu/, https://cosmicrays.oulu.fi/)

6.1 GCR diurnal anisotropy

Assessment of cross-correlation based on one-minute count rates from pairs of NMs having similar cutoff rigidities and various asymptotic longitudes was presented as an alternative for the diurnal anisotropy measurement technique [76].

Consideration of the GCR diurnal anisotropy properties emphasized the importance of properly taking into account the temperature effect in MDs data [77].

It was reported that Dome C NM is hardly sensitive to the GCR diurnal anisotropy having amplitudes at the level of 0.03% (other polar NMs exhibited amplitudes from 0.16 to 0.4%). This effect was explained by a narrow asymptotic-direction cone of Dome C NM looking nearly to the South pole, accepting cosmic-ray particles originating from the off-equatorial region [78].

There was also presented a data-mining approach for the GCR anisotropy study [79].

Studies of the GCR diurnal anisotropy long-term changes allows to consider role of the solar wind velocity, as well as HMF on this variability [80-82]. Temporal behavior of the third harmonic and tridiurnal of GCR anisotropy was discussed [83-84].

Based on estimations of the GCR diurnal anisotropy it was postulated that in positive polarity epochs a diffusion model of GCR heliospheric transport with noticeably manifested drift is acceptable. Whereas the diffusion-dominated model is more acceptable during the negative polarity epochs. Moreover, magnitudes of the radial and tangential anisotropy components at different HMF sectors were used to calculate the GCR modulation parameters [85].

6.2 Forbush decreases

Features of Forbush decrease (Fd) registered in March 2012 by the Latin American Giant Observatory (LAGO) were discussed [86]. Also Fds properties, visible in the electrons precise measurements in the period 2017-2021 of the Dark Matter Particle Explorer (DAMPE) were discussed [87]. The observations of the Forbush decreases made by the Alpha Magnetic Spectrometer (AMS-02) on the board of the International Space Station from 05.2011 to 10.2019 were discussed [88]. Authors presented various characteristics of Fds, such as Fds rigidity dependence.

6.3 Mid-term GCR periodicities

PAMELA and ARINA spectrometers measurements allowed for examination of the time profiles and the rigidity dependence of the recurrent variations observed in a broad range of energy, directly in space [89]. Authors presented that the GCR 27-day variation amplitude cannot be described by the same power-law at both high and low energies.

Analysis of 48 years of the Nagoya muon telescope data revealed a new periodicity of 125 ± 45 days [90].

6.4 Long-term GCR variations

The CALorimetric Electron Telescope (CALET) onboard the International Space Station measurements of electron and proton count rates during the period of 10.2015-04.2023 showed a clear charge-sign dependence of the GCR solar modulation [91]. Authors stated that the drifts play a major role in the GCRs long-term modulation.

The solar modulation potential reconstruction ϕ, based on the daily AMS-02 data, was reported. The comparison with ϕ obtained from NMs data showed a good agreement (for lower energy boundary equal 3 GeV) [92].

7. Solar modulation of GCR modeling

Various subjects concerning modeling of the galactic cosmic rays transport in the heliosphere, based on the Parker transport equation [93] were reported.

Drift effects, as well as, the heliospheric current sheet (HCS) variation in the 22-year solar magnetic cycle of GCR and anomalous cosmic rays (ACRs) modulation were modeled, addressing especially the question how does ACR acceleration at the termination shock change during the magnetic cycle, and how does waviness of HCS impacts the acceleration process [94].

Presented results of the GCR transport modeling with computed radial and latitudinal gradients, as well as proton energy spectra reproduced well Ulysses and PAMELA measurements [95].

Mathematical modeling comparing GCR modulation during the recent two solar minima: 2009 (A<0) and 2020 (A>0) exhibited that the only differences incorporated into the modeling between these minima was the corresponding tilt angles of the HCS together with the sign and magnitude of the HMF. Moreover, it was shown the necessity of additional reduction of the latitudinal enhancement of perpendicular diffusion coefficient by a factor of 2 in order to properly reproduce the HEPD01 proton spectrum in 2020 [96].

Modeling results based on the solutions of 3-D Parker's GCR transport equation were reported. It was demonstrated that there is a need of including into the model heliolongitudinal

asymmetry of the solar wind velocity and HMF in order of gaining a reliable and realistic results [97].

Usage of the 3D drift model of temporal modulation of galactic protons to compute proton spectra from 2009 to 2019, with changing solar activity levels, in comparison with observations from PAMELA and AMS02 was reported [98]. PAMELA and AMS observed a significant temporal changeability in the p/He ratios at rigidities below 3 GV. Attempts to explain this phenomenon using GCR transport modeling have been presented [99-100]. Steady state Parker transport equation with neural networks accelerator were discussed [101]. Interplanetary scintillations were used as a proxy of solar wind speed latitudinal profile, with an uncertainty around 50 km/s [102]. Presented results were compared with the PAMELA and AMS 2 observations.

Stochastic differential equations approach to the GCR heliospheric transport modeling with the CUDA programming language used, allowed to speed-up the computations of the orders of $\sim 10-40\times$ [103]. A new tool for GCR transport simulations: CudaHelioCommander was presented. It was used for testing a uniqueness of the Parker transport equation solution of the in 1D and 2D space [104]. GCR modulation during the descending phase of the SC 24 was discussed in the updates of the HelMod-4 parametrization [105]. The HelMod model is based on the Monte Carlo simulation evaluating GCR transport in the heliosphere. It reproduces modulated spectra of protons, helium, heavier species as Carbon, Oxygen, etc., antiprotons and electrons showing a good agreement with high-precision AMS-02 data.

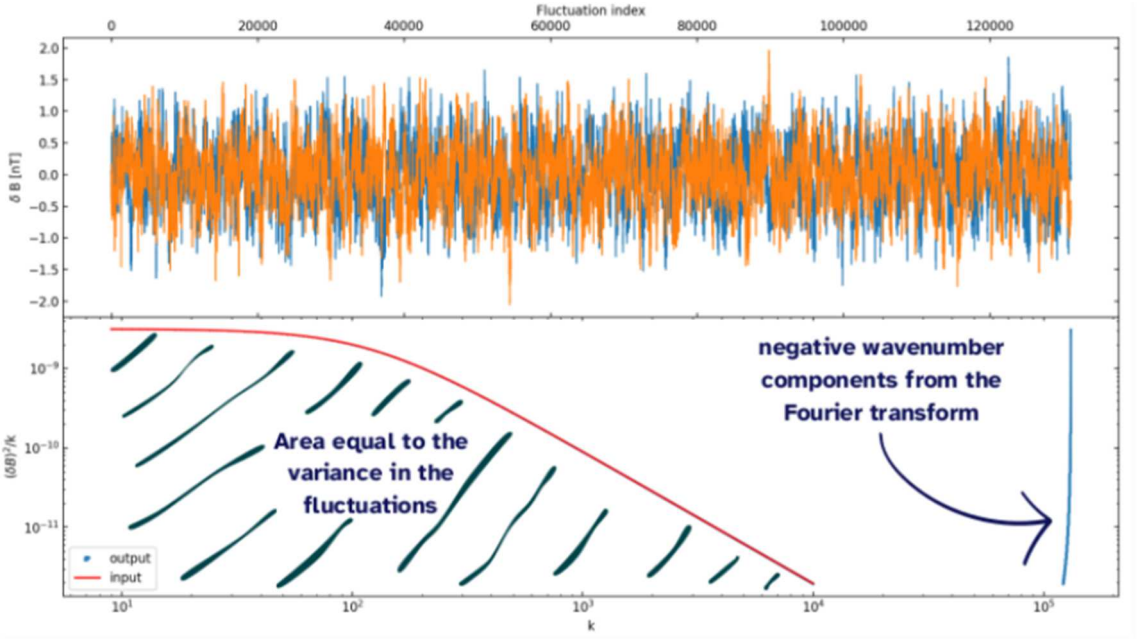

Figure 8. The 1D slab synthetic turbulence component along with the corresponding power spectrum-the example [107].

Substantial progress taking place in turbulence modeling and particle scattering theories, along with advancements in observations, has enabled the more realistic and correct modeling of cosmic ray diffusion and drifts [106]. And this in turn has resulted in the development of increasingly intricate CR transport models. Also, a usefulness of an ab initio approach allowing

to avoid ambiguities in empirical model parameters was. And this in turn has resulted in the development of increasingly intricate CR transport models. The Author has also raised several unresolved issues of GCR heliospheric transport.

Charged particle transport in the presence of realistic synthetic turbulence was studied. There was reported the influence of a strong slab turbulence on the diffusion coefficients: parallel and perpendicular, as well drift coefficients [107].

An alternative approach was presented for the calculation of the pitch angle scattering of energetic charged particles in stochastic magnetic fields. Shear is present almost everywhere, and might play an important role close to perpendicular pitch angles that is a sore point of the QLT [108].

Combined MHD and GCR transport model with diffusion coefficients for protons and helium was presented [109]. Simulations showed that the effect of CIR on protons is weaker than for 4He, but stronger than 3He. As a possible cause was stated that their mass to charge ratios are different. Global magnetohydrodynamic (MHD) simulations with the test particle simulation with steady solar wind and no pitch angle scattering were delivered [110]. The statistical behavior of $\sim$ 10 GeV and $\sim$ 1 TeV protons arriving deep inside the virtual heliosphere was different. Lower energy particles arrive in the mid-high latitude region of the inner boundary, while for the higher energy GCR particles they tend to arrive at the mid-low latitude of the tail region.

The GCRs modulation near heliopause with the effect of a boundary layer beyond heliopause was simulated giving a good agreement with the Voyager 2 observations [111].

Physical processes affecting the transport of GCRs from the LISM into the heliosphere were discussed. It was emphasized that while it is clear that GCRs of moderate energy are disturbed by the presence of the heliosphere, even GCRs in the TeV-PeV energy range are influenced. This means that any theoretical explanation of their behavior requires subtracting the heliospheric influence from air shower observations [112]. Quantitative study of the origin of TeV cosmic rays anisotropy, based on the data of Tibet ASγ and MHD model were presented [113]. The relative intensity distribution of cosmic rays at the outer boundary of the heliosphere containing small-scale anisotropic features was noticed.

Mathematical model of the astrospheric transport of GCRs in 3D for Proxima Centauri b, with termination shock located at 76 AU, with constant solar wind speed of 1500 km/s, Parker field at the level of 1.8 nT and SW density 0.25 /cc at 1 AU, was discussed [114]. Additionally, stellar rotation rate was taken 82.6 days.

8. Summary

- Well-situated, ground-based, covering a wide range of energies, observatories, such as NMs, MTs, etc., make possible detection and forecasting of space weather phenomena. They contribute to the deepening of our knowledge about the complex, near Earth, radiation environment.
- There is a need of learning about the solar and heliospheric unknown properties by space probes.
- We need precise models of SEP acceleration and transport, not only in the vicinity of the Earth, but also in regions closer to the Sun, where PSP or SolO are currently observing and will

observe them, where acceleration processes have not had the opportunity to fully develop and particles injection is in progress.

- We need accurate models of GCR heliospheric transport at various time and energy scales.
- GCR measurements on the ground alone, as well as in-situ alone, are not enough for understanding heliospheric transport and acceleration processes.

Acknowledgements:

To all outstanding Authors of talks and posters for fantastic presentations and discussions. ICRC 2023 LOC for organizing such a successful conference.

References

[1] Cohen C. for the Parker Solar Probe and Solar Orbiter Energetic Particle Teams, Close Encounters of the Solar Kind, these proceedings

[2] Müller D., Cyr, Zouganelis, et.al., The Solar Orbiter mission: Science overview, A&A 642, A1 (2020), https://doi.org/10.1051/0004-6361/202038467

[3] Fox N., Velli, Bale, et al., The Solar Probe Plus Mission: Humanity's First Visit to Our Star. Space Sci Rev 204, 7–48 (2016). https://doi.org/10.1007/s11214-015-0211-6

[4] Cohen C.,Christian, Cummings, et al., Parker Solar Probe Energetic Particle Observations of the September 5, 2022 SEP Event, these proceedings

[5] Leske R.,Christian, Cohen, et al., Observations of Extremely 3He-Rich Solar Energetic Particle Events from Parker Solar Probe, these proceedings

[6] Labrador A., Mitchell, Christian, et al., Observations of High Energy Electrons during the 5 September 2022 Solar Energetic Particle Event with the Parker Solar Probe EPI-Hi Instrument, these proceedings

[7] Consolandi C., on behalf of the AMS collaboration, Solar Energetic Particles measured by the Alpha Magnetic Spectrometer, these proceedings

[8] Palma F., Martucci for the Limadou/HEPD-01 Collaboration, Review of magnetospheric and space weather observations by the High-Energy Particle Detector (HEPD-01) on board the CSES-01 satellite, these proceedings

[9] Martucci M. for the Limadou/HEPD-01 Collaboration, Solar physics between the 24th and 25th solar cycles: observations and results from the High-Energy Particle Detector (HEPD-01) onboard the CSES-01 satellite, these proceedings

[10] Nicolaidis R., Gebbia, Iuppa, et al. for the CSES-Limadou collaboration, The TDAQ system of the HEPD-02 on the CSES-02 mission, these proceedings

[11] Sparvoli R., The CSES multi-satellite programme, these proceedings

[12] Kazutaka Y., Tajima, Miyata,et al., SOlar Neutron and Gamma-ray Spectrometer (SONGS), these proceedings

[13] Liu W., Jiang, Wu, et al., Research on the On-orbit Background of the Hard X-Ray Imager Onboard ASO-S, these proceedings

[14] Jiang X., Zhang, Chen, et al., The collimator of the Hard X-ray Imager: Mathematical model and Experimental validation, these proceedings

[15] Martin S., Clem, Evenson, et al., Geomagnetic Diurnal Transitions of Positron and Electron Flux at 20 – 300 MeV as Observed by the AESOP-Lite Balloon Payload, these proceedings

[16] Simpson, J. A. 2000, Space Sci. Rev., 93, 11

[17] Bindi V, Consolandi, Ryan, et al., Haleakala Neutron Monitor Redeployment, these proceedings

[18] Muangha P., Ruffolo, Sáiz, et al., Comparison of Cosmic Ray Spectral Variation during 2015-2019 as Indicated by the South Pole Neutron Monitor Leader Fraction and AMS-02 Spectral Index, these proceedings

[19] Siluszyk M., Iskra, Wozniak, On the Rigidity Spectrum of Galactic Cosmic Ray Intensity Variations in 24 Solar Cycle, these proceedings

[20] Evenson P., Clem, Mangeard, et al., Neutron Monitor as a Calorimeter to Measure Particle Spectra, these proceedings

[21] Madlee S., Ruffolo, Sáiz, et al., Monte Carlo Simulation of the Neutron Monitor and Position-Dependent Bare Neutron Counter Yield Functions at Mawson Station, Antarctica, these proceedings

[22] Poopakun K., Nuntiyakul, Khamphakdee, et al., Solar Magnetic Polarity Effect on Neutron Monitor Count Rates: Comparing Latitude Surveys and Antarctic Stations, these proceedings

[23] Seripienlert A., Nuntiyakul, Khamphakdee, et al., Simulations of the Yield Functions of a Semi-Leaded Neutron Monitor from Latitude Surveys, these proceedings

[24] Chaiwongkhot K., Ruffolo, Sáiz, et al., Measurement of sparse vs. dense atmospheric secondary particles from cosmic ray showers using coincident signals on various counters in a neutron monitor, these proceedings

[25] Sáiz A., Ruffolo, Sukha, et al., Cross-counter time-delay distributions at the Mawson neutron monitor, these proceedings

[26] Heifner C., Nuntiyakul, Puyleart, et al., Neutron Bursts from Air Showers in Ice: Implications for Neutron Detection with the South Pole Neutron Monitors, these proceedings

[27] Pagwhan A., Seripienlert, Nuntiyakul, et al., Monte Carlo Simulations of South Pole Neutron Monitor Counting Rate since 1964, these proceedings

[28] Kittiya A., Nuntiyakul, Seripienlert, et al., Cosmic Ray Flux Correlation between McMurdo and Jang Bogo Neutron Monitor, these proceedings

[29] Evenson P., Clem, Mangeard, et al., New Boron Trifluoride proportional tube for the NM64 Neutron Monitor, these proceedings

[30] Blanco J., García-Tejedor, García-Población, et al., Izaña Cosmic Ray Observatory, these proceedings

[31] Monterde-Andrade F., González, Valdés-Galicia, et al., Preliminary Simulation of the Scibar Cosmic-Ray Telescope (SciCRT) at Sierra Negra, these proceedings

[32] Newton-Bosch J., González, Valdés-Galicia, et al., Geomagnetic Storm Effects on the Solar Neutron Telescope at Sierra Negra, Mexico, these proceedings

[33] Muraki Y., Miyake, Koi, et al., Proton Penetration Efficiency over Sierra Negra (Mexico) and Oulu (Finland), these proceedings

[34] Vigorito C., Vernetto, Bedogni, et al., for the SAMADHA collaboration, SAMADHA neutron spectrum and cosmic ray dose rate measurements at 5200 m in the SAA region, these proceedings

[35] Hariharan B., Chakraborty, Dugad, et al., The potential role of GRAPES-3 experiment in space weather forecasting, these proceedings

[36] Oshima A., Tanaka, Kojima, et al., The Akeno Muon Observation: A Joint Research for Near Earth Space by Japan-India Collaboration, these proceedings

[37] Koennonkok K., Ruffolo, Mitthumsiri, et al. on behalf of the LHAASO Collaboration, Hourly measurement of cosmic ray anisotropy by LHAASO WCDA at ∼1 TeV: Effects of an interplanetary flux rope during 2021 November, these proceedings

[38] Otiniano, Response of a Modular Scintillator Detector to Cosmic Ray Muons, these proceedings

[39] Tsuchiya H., Wada, Enoto, et al., Observation of a downward terrestrial gamma-ray flash and the flash-induced neutrons, these proceedings

[40] Kóta J., Puzzoni, Fraschetti, TeV Cosmic Rays Around the Sun: Sun's Shadow and Solar Gamma Rays, these proceedings

[41] Nan Y., Chen, Feng for the LHAASO Collaboration, Measurement of the Daily Interplanetary Magnetic Field Using the Cosmic-ray Sun Shadow by LHAASO-KM2A, these proceedings

[42] Orlando E., Petrosian, Strong, A New Component from the Quiet Sun: Synchrotron Radiation from Galactic Cosmic Rays from Radio to Gamma, these proceedings

[43] Mauro J., de Wasseige on behalf of the KM3NeT Collaboration, Improving the sensitivity of KM3NeT to MeV-GeV neutrinos from solar flares, these proceedings

[44] Masuda Y., Kato, Hayashi, et al. for the GMDN collaboration, Galactic cosmic ray variations associated with February 2022 "Starlink" magnetic storms observed with global networks of neutron monitors and muon detectors, these proceedings

[45] Gil A., Berendt-Marchel, Modzelewska, et al., Indications of geoeffective space weather events in cosmic rays observed during the rising period of the solar cycle 24, these proceedings

[46] Hayashi Y., Kato, Masuda, et al. for the GMDN collaboration, Cosmic ray variation caused by coronal mass ejections without direct impact on Earth, these proceedings

[47] Blanco J., Arrazola, Hidalgo, Interplanetary Coronal Mass Ejection of October 3, 2021, these proceedings

[48] Asorey H., Suárez-Durán, Mayo-García, ACORDE: A new method to calculate onboard radiation doses during commercial flights, these proceedings

[49] Larsen N., Mishev, Usoskin, Investigating the Relationship Between GLE Neutron Monitor Data and Radiation Dose at Flight Altitudes, these proceedings

[50] Larsen N., Mishev, Usoskin, Using a Modern Radiation Dose Model to Investigate Exposure Rates During GLE 73, these proceedings

[51] Mishev A., Larsen, The Easter GLE on 15 April 2001, spectra and angular distribution–new revised results and related space weather effects, these proceedings

[52] Larsen N., Mishev, Usoskin, Development of a new Open-Source Tool for Computing Cosmic Ray Trajectories in the Earth's Magnetosphere (OTSO), these proceedings

[53] Huo R., Astronaut Radiation Dose Calculation with a New Galactic Cosmic Ray Model and the AMS-02 Data, these proceedings

[54] Benella S., Laurenza, Plainaki, et al., A comprehensive study of solar energetic particle propagation during the first ground-level enhancement of the solar cycle 24, these proceedings

[55] Mekhaldi F., Muscheler, Adolphi, et al., Multiradionuclide evidence for the solar origin of the cosmic-ray events of AD 774/5 and 993/4, Nat. Commun. 6 (2015) 8611

[56] Koldobskiy S., Mekhaldi, Kovaltsov, et al., Reconstruction of the fluence of extreme solar particle events registered in cosmogenic proxies, these proceedings

[57] Mishev A., Usoskin*a*, Panovska, Extreme solar particle event of 774 AD: reference as the worst-case scenario for space weather, these proceedings

[58] Miyake F., Hakozaki, Hayakawa, et al., Investigation of extreme solar events in the 19th century from tree ring 14 C data, these proceedings

[59] Hayakawa H., Mishev, Koldobskiy, et al., Digitizations of Historical Solar Cosmic-Ray Measurements for the GLE 1 – 4, these proceedings

[60] Mishev A., Hayakawa, Usoskin, et al., Spectra and anisotropy during GLE # 4 on 19 November 1949 derived using historical records, these proceedings

[61] Modzelewska R., Ahluwalia, Kota, Galactic cosmic ray modulation in the heliosphere based on muon telescopes and ion chambers data, these proceedings

[62] Poluianov S., Batalla, Mishev, et al., Two sub-GLE events detected with South Pole and Vostok neutron monitors in 1968 and 1969, these proceedings

[63] Usoskin I., Koldobskiy, Pouianov, et al., Consistency of the average flux of solar energetic particles over different timescales up to mega-years, these proceedings

[64] Raukunen O., Usoskin, Koldobskiy, et al., New reconstruction of annual integral solar proton fluences between 1984- 2019, these proceedings

[65] Mauro J., de Wasseige, Searching for sub-populations within the gamma-ray solar flares catalog: a graph-based clustering analysis, these proceedings

[66] Wang Y., Qin, The Crucial Role of Perpendicular diffusion in the Longitude Distribution of > 10 MeV Solar Energetic Protons, these proceedings

[67] Zhang M., Cheng, Simulation of solar energetic particle events with a data-driven physics-based transport model, these proceedings

[68] Li G., Jin, Ding, Modelling Gradual Solar Energetic Particle Events Using the SEPCaster Model, these proceedings

[69] Fraschetti F., Goldberg, Modeling flat proton spectra at large solar energetic particle events at 1 AU via particle escape into a self-generated/pre-existing turbulence, these proceedings

[70] Particles Acceleration on Flare Termination Shock, Wang X., Feng, Yan, et al., these proceedings

[71] Wang X., Yan, Feng, et al., Particles Acceleration on Twin-shock of Solar Flare Jets, these proceedings

[72] Ruffolo D., Sonsrettee, Chuychai, et al., Magnetic field line path length variations and effects on solar energetic particle transport, these proceedings

[73] Otsuka F., Matsukiyo, Ok, Shock parameter dependence of electron acceleration at quasi-perpendicular collisionless shock, these proceedings

[74] Wang W., Wang, Krucker, et al., Energy Spectrum of Solar Energetic Electron Events Over 25 Years, these proceedings

[75] Wu X., Li, Zhao, et al., Statistical study of release time and its energy dependence of in-situ energetic electrons in impulsive solar flares, these proceedings

[76] Sonsrettee W., Nuntiyakul, Seripienlert, et al., Time Lag in Diurnal Correlations vs. Asymptotic Longitudinal Separation, these proceedings

[77] Munakata K., Kozai, Kato, et al., Analysis of temporal variation of cosmic ray intensity observed with global networks of neutron monitors and muon detectors, these proceedings

[78] Gil A., Mishev, Poluianov, et al., Diurnal variations of galactic cosmic rays as detected by polar neutron monitors, these proceedings

[79] Kozai M., Hayashi, Kato, et al., Data mining of cosmic-ray anisotropy observed with the Global Muon Detector Network, these proceedings

[80] Zuberi M., for the GRAPES-3 collaboration, Study of modulation cycles of cosmic ray diurnal anisotropy variation using 22 years of GRAPES-3 muon data, these proceedings

[81] Koi T., Kojima, Shibata, et al., Dependence of solar diurnal variation on solar wind speed, these proceedings

[82] Kojima H., Shibata, Takamaru, et al., Solar wind velocity dependence of the flow of galactic cosmic rays perpendicular to the ecliptic plane on the polarity of the interplanetary magnetic field, these proceedings

[83] Richharia M., Eleven year variation in third harmonics of daily variation in cosmic ray intensity on quiet days at worldwide network of neutron monitoring, these proceedings

[84] Richharia M., Chouhan, Effect of solar poloidal magnetic field reversal on tridiurnal anisotropy of cosmic ray intensity on quiet days at different latitude neutron monitoring stations, these proceedings

[85] Iskra K., Modzelewska, Siluszyk, et al., On the Anisotropy of Galactic Cosmic Ray focus on 1996 to 2020, these proceedings

[86] Otiniano L., New Analysis of Forbush Decrease Detected by a single LAGO Water Cherenkov Detector, these proceedings

[87] Li W., Zang, Yuan, et al., for the DAMPE collaboration, A study of Forbush Decreases effects with DAMPE experiment, these proceedings

[88] Wang S., Bindi, Consolandi, et al., Properties of Forbush Decreases observed with the AMS-02 daily proton flux, these proceedings

[89] Modzelewska R., Bazilevskaya, Boezio, et al., on behalf of PAMELA collaboration, Study of 27-day variations in the GCR fluxes in 2007-2008 based on PAMELA and ARINA observations, these proceedings

[90] Muraki Y., Shibata, Takamaru, et al., The 48 year data analysis of Nagoya muon telescope- Discover of (125± 45) day periodicity, these proceedings

[91] Miyake S., Munakata, Akaike, for the CALET collaboration, Cosmic-Ray Modulation during Solar Cycles 24-25 Transition Observed with CALET on the International Space Station, these proceedings

[92] Koldobskiy S., Usoskin, Reconstruction of solar modulation potential from AMS-02 daily data for the period 2011 – 2019 and its comparison with indirect cosmic-ray measurements, these proceedings

[93] Parker E.N., Planet. Space Sci. (1965) 13, 9 – 32

[94] Kóta J., Solar Cycle Variation of Anomalous and Galactic Cosmic Rays: The Role of Drifts and Current Sheet, these proceedings

[95] Luo X., Geng, Potgieter, et al., A numerical study of the cosmic ray latitudinal and radial gradients in the heliosphere, these proceedings

[96] Ngobeni M., Aslam, Potgieter, et al., Modelling the modulation of galactic protons in two successive very quiet solar minima, these proceedings

[97] Gil A., Modzelewska, The impact of diffusion and convection on the recurring variability of galactic cosmic rays, these proceedings

[98] Ndiitwani D., Aslam, Ngobeni, et al., The 3D numerical modelling of the temporal modulation of galactic protons as per PAMELA and AMS02 observations with changing solar activity, these proceedings

[99] Ngobeni M., Aslam, et al., Towards understanding of the time dependence of the proton to helium ratios in the heliosphere, these proceedings

[100] Song X., Implication of the time variation of galactic cosmic ray proton-to-helium flux ratio, these proceedings

[101] Corti C., Sadowski, Nikonov, et al., Constraining the global heliospheric transport of galactic cosmic rays in solar cycles 23 and 24, these proceedings

[102] Sokół J., Bzowski, Tokumaru, et al., Sol Phys 285, 167–200 (2013), https://doi.org/10.1007/s11207-012-9993-9

[103] Della Torre S., Cavallotto, Besozzi, et al., Advantages of GPU-accelerated approach for solving the Parker equation in the heliosphere, these proceedings

[104] Nguyen M., Bobík, Genči, The uniqueness of the Parker equation solution, these proceedings

[105] Boschini M., Della Torre, Gervasi, et al., Predicting galactic cosmic ray intensities in the heliosphere employing the HelMod-4 model, these proceedings

[106] Engelbrecht E., Aspects of Cosmic Ray Transport Theory in the Heliosphere, these proceedings

[107] Els P., Engelbrecht, Testing numerical accuracy of particle pushers by means of 1D synthetic turbulence, these proceedings

[108] Kóta J., Quasi Linear Theory of Pitch-angle Scattering: an Alternative Formulation, these proceedings

[109] Luo X., Potgieter, Zhang,et al., A Numerical Study of the Effects of a Corotating Interaction Region on Cosmic-Ray Transport: Some features of different Cosmic-Ray Composition and Rigidity, these proceedings

[110] Yoshida K., Matsukiyo, Washimi, et al., Effects of heliospheric boundary structures on galactic cosmic ray transport: Global MHD and large-scale test particle simulations, these proceedings

[111] Gou X., Numerical Simulation of Galactic Cosmic Rays Modulation near Heliopause and its Comparison with Voyager 2 Observation, these proceedings

[112] Pogorelov N., Cummings, Fraternale, et al., Solar Wind Interaction with the Local Interstellar Medium: Its Role in the Galactic Cosmic Ray Modulation, these proceedings

[113] Sako T., on behalf of the Tibet ASγ collaboration, Pogorelov, Modeling of the galactic cosmic-ray anisotropy at TeV energies using an intensity-mapping method in an MHD model heliosphere, these proceedings

[114] Engelbrecht N., Scherer, Light, et al., On the 3D transport of galactic cosmic rays in exoplanet-hosting astrospheres: a case study of Proxima Centauri b, these proceedings